Effect of CNT on the Mechanical Property of Graphene/Epoxy Composite by Molecular Dynamics Simulations

Zhikun Wang[1, 2, a], Shuangqing Sun[1, 2, b], Songqing Hu[1, 2, c, *]

[1]School of Materials Science and Engineering, Qingdao 266580, China

[2]Institute of Advanced Materials, China University of Petroleum (East China), Qingdao 266580, China

[a]wzhikun0806@163.com, [b]sunshuangqing@upc.edu.cn, [c]songqinghu@upc.edu.cn

*Corresponding author

Keywords: Carbon nanotube, Graphene, Epoxy, Composite, Molecular dynamics simulations

Abstract: Molecular dynamics simulations were adopted to explore the effect of carbon nanotube (CNT) on the mechanical property of graphene/epoxy composite. Emphasis was laid on investigating the variation of CNT length and relative distance between CNT and graphene on the composite property. The stress-strain curves and Young's moduli of the composite along axial and radial directions of CNT were obtained, which indicate that the existence of CNT, as well as the increase of CNT length and CNT-graphene separation within a limited distance, can enhance the mechanical property of the composite. This is mainly attributed to the formation of an interfacial adsorption layer of epoxy segments near CNT and graphene surfaces, as well as the π-π interaction between benzene rings. Interaction energy variation between graphene and CNT/epoxy (or CNT) versus CNT length, and morphological fracturing process of the composite, further highlight the significance of the interfacial adsorption region on improving the mechanical property of the composite on both axial and radial directions of CNT.

1. Introduction

Carbon nanotubes (CNT) and graphene have aroused widespread interests due to their excellent mechanical, thermal and electromagnetic properties. Based on these properties, the two carbon materials have been used as nanofillers in modifying the overall performance of polymeric materials [1]. Obtained composites show remarkable enhanced property when appropriate size, content, dispersion states of the nanofillers are selected. Considering differences between CNT and graphene in shape, researchers recently focus on the synergetic effect between the two carbon materials in improving the property of the composite in microscopic molecular scale [2, 3].

Yang and Sumfleth [4, 5] proved the synergistic effect of CNT/graphene on enhancing the mechanical property of a polymer matrix. Kim and Zhang [6, 7] highlighted the importance of CNT and graphene dispersion on the overall property of composites. Previous experiments contributed the synergetic effect of CNT and graphene to the improved dispersion of them in polymer matrix, as well as the enhanced interfacial adhesion behavior between the nanofillers and the matrix [8-15]. However, these discussions are rarely performed in molecular level, and direct observations in microscopic scale on the synergetic effect are needed.

Molecular dynamics (MD) simulations have shown great potential in revealing dynamical and structural properties of nanocomposite materials in molecular level. Liu [16] performed MD simulations on the interfacial interactions between CNT/graphene and polyethylene molecules, and found that a large interfacial adhesion force needs particular selection of the radius, length, and distribution of CNT and graphene. Zhang [17] focused on the tensile process of composite materials by MD simulations, and found that the relative location of CNT and graphene can influence the failure behavior of the composite during external stretching.

Here, we focus on the synergistic effect of CNT and graphene on modifying the mechanical property of an epoxy matrix. Molecular interactions in the interfacial adsorption region between

CNT/graphene and epoxy matrix have been investigated. A gradual tensile process has been adopted to simulate the mechanical property of the composite model. The effects of CNT length and distance between CNT and graphene on the overall property are analyzed.

2. Methods

2.1 Modeling details

We chose diglycidyl ether of bisphenol A (DGEBA) as epoxy monomer and cyclohexylamine (CHA) as linker. A copolymerized chain DGEBA– CHA–DGEBA–CHA was used to construct the epoxy matrix ($1.12 g/cm^3$). A graphene sheet with size of 43.46×43.79 Å^2 and a CNT with varied lengths were added into the epoxy matrix. The size of the composite model is 46.00^3 Å^3. We use Materials Studio software to construct the model and perform all simulations. COMPASS force field was used to describe intra- and inter- molecular interactions within the model [18-22]. Ewald and atom-based summation methods were used for Coulomb and van der Waals interactions, respectively. The composite model was first relaxed by a geometry optimization process, then equilibrated by a 2ns MD simulation at 400K, during which the relative location of CNT and graphene was fixed. Then, a 4ns MD simulation at 300K was performed for the production run. NVT ensemble was used for MD simulations. Time step was set to 1fs.

2.2 Uniaxial tensile simulations

Fig. 1 indicates the uniaxial tensile method of the composite model. The simulation is performed based on an algorithm in perl script. For tension on the axial direction of CNT, the largest strain of the composite is 1.5% and the single tension step is 0.1%, leading to a total of 15 stretching stages. At each step, geometric optimization and MD simulations (200ps) are used to equilibrate the model. To calculate the average stress of the composite during stretching, the last 50ps of the trajectory are averaged. Stress and strain of the model are extracted for the stress-strain curve. For tension on the radial direction of CNT, similar stretching procedure and data processing method are used. The differences are that the total uniaxial tension strain in the radial direction of CNT is 30%, and the single step tension ratio is 1%.
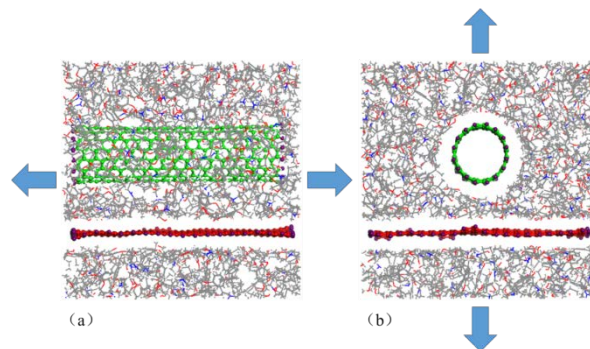

Figure 1. Uniaxial tension methods. (a) axial, (b) radial

3. Results and discussion

3.1 Tensile simulations on axial direction of CNT

To study the tensile properties of composites on the axial direction of CNT, a series of composite models with different lengths of CNT were constructed (Fig. 2). The tensile tests and analysis were carried out through a uniaxial tensile algorithm based on perl script.
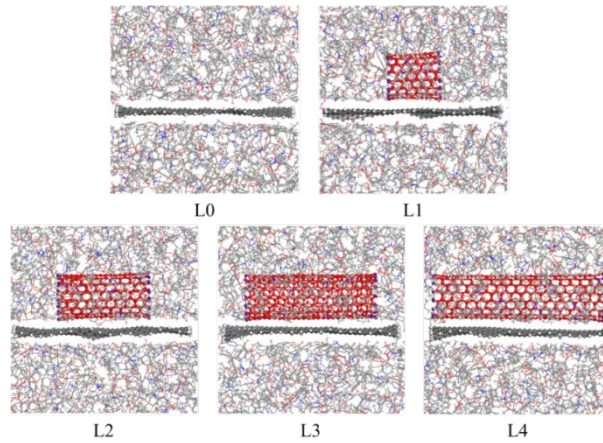
Figure 2. Models with various CNT lengths. L0 to L4 are 0, 13.03, 22.87, 32.70, 42.54 Å, respectively
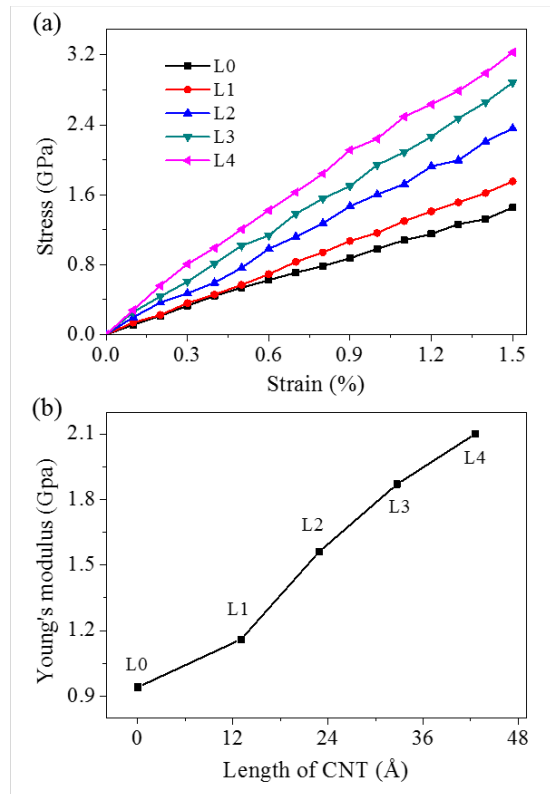

Figure 3. Stress-strain curves (a) and Young's moduli (b) of composites at different CNT lengths

Fig. 3 shows the stress-strain curves and Young's moduli of CNT/graphene/epoxy composites in the axial direction of CNT. The effect of CNT length on the tensile properties of composites was studied. Since the total uniaxial tensile strain is 1.5%, the composite is in the state of elastic deformation within this strain range. The stress and strain obey Hooke's law, showing a linear relationship. It can be seen from the slopes in Fig. 3a that the mechanical property of the composite on the axis of CNT has been improved after the addition of CNT, and with the increase of the CNT length, the mechanical property increases. By linear fitting of the stress-strain curves in Fig. 3a, the Young's moduli of composites are obtained, as shown in Fig. 3b. Without addition of CNT in the composite, that is, the length of CNT is 0, the Young's modulus of the graphene/epoxy composite is 0.94 Gpa. When the CNT length is 42.54 Å, the Young's modulus increases to 2.10 Gpa. As epoxy materials contain a large number of benzene rings and epoxy groups, there will be an adsorption layer of epoxy segments near graphene and CNT, and special interfacial regions will be formed. Researchers have reported that molecular chains in the interfacial adsorption layer have higher

density and weaker dynamical properties than those in the bulk region. Therefore, the interfacial adsorption layer on CNT surface has better mechanical property and increases at larger CNT length. When composites are subjected to stress on the CNT axis, the mechanical property of CNT/graphene/epoxy composite is enhanced.

To study the effect of CNT length on the binding property of graphene, the interaction energy between graphene and matrix (epoxy or epoxy+CNT) was studied (Fig. 4). The diameter of CNT is d = 10.85 Å. CNTs are parallel and 3.4 Å away from the graphene surface. The interaction energy between graphene and matrix is negative, representing attractive forces between then. The L0 model represents the case when CNT is not added. Compared with the interaction energies of systems containing CNT, the binding strength of graphene and matrix is the weakest. Thus, the addition of CNT improves the binding effect of graphene in composites. With the increase of CNT length, the interaction energy decreases gradually in an almost linear trend. We conclude that the longer the CNT is, the better the binding effect of graphene in composite will be. In Fig. 4b, the interaction energy between graphene and CNT increases with the increase of CNT length, indicating that the binding effect between graphene and CNT can be enhanced at longer CNT. Linear fitting of the curve shows that the interaction energy between graphene and CNT varies linearly versus CNT length in form of $\Delta E = -6.461 \times L_{CNT} + 4.522$ (kcal/mol). The vdW force between ring structures on graphene and CNT leads to the strong intermolecular attraction between the two nanofillers, and with increasing CNT length, the attraction force becomes stronger. Through above analyses, it is concluded that the addition of CNT can improve the thermal stability of graphene in composites.
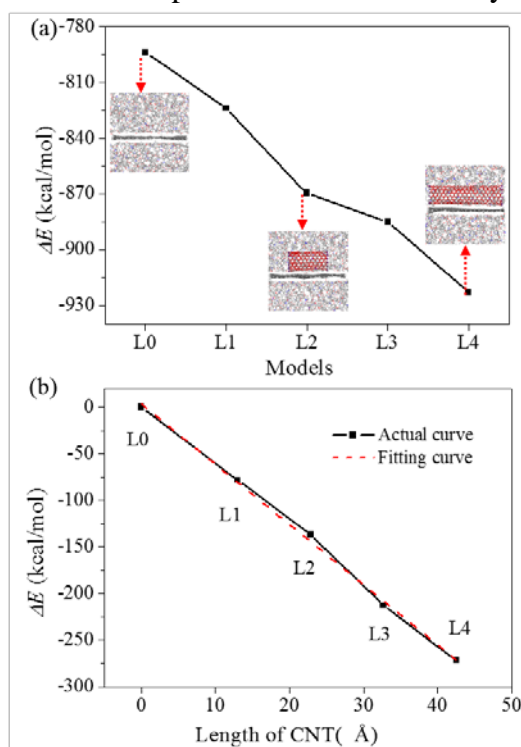

Figure 4. Interaction energy between graphene and CNT/epoxy (a) or CNT (b) versus CNT length

3.2 Tensile simulations on radial direction of CNT

Fig. 5 shows the stress-strain curves of CNT/ graphene/epoxy composites under radial tension. The distance between CNT and graphene changes from 1d to 2d and 3d (d = 3.4 Å) in three models. The effect of dispersion between CNT and graphene on the mechanical property of the composite is investigated. It can be seen from the figure that the composite model has experienced elastic stage, micro-plastic stage, yield stage and softening stage during the stretching process. After 3% of the strain the three models basically reach the yield stage, and the mechanical properties of the composites decrease significantly with further increase of the strain. By comparing the three stress-strain curves, we find that the greater the distance between CNT and graphene, the better the

mechanical property of the composite in the radial direction of CNT will be. In other words, the increased dispersion degree between CNT and graphene has the ability to improve the mechanical property of the composite. This is mainly attributed to the formation of the interfacial adsorption layer between CNT and graphene at larger d.
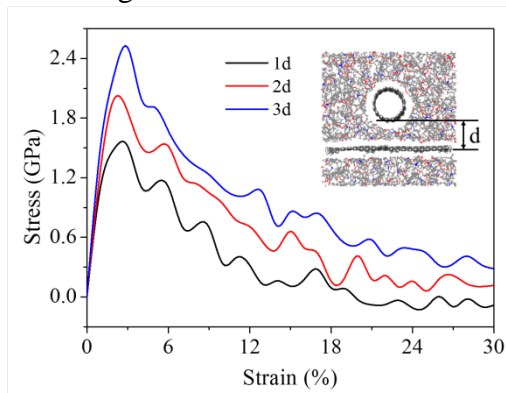

Figure 5. Stress-strain curves of composites during uniaxial tensile simulation

Fig. 6 is the configuration diagram of the model during the tensile process. With the increase of tensile strain, the voids in the composites gradually increase, and eventually the epoxy matrix and nanofillers are separated, resulting in the failure of materials. In contrast to the non-tensioned model, the overall configuration of the composite does not change significantly at 3% strain. From the stress-strain curve of Fig. 4, it can be seen that the composite model is in the stage of micro-plasticity. Since the overall stress variation of the model is uniform, there is no stress concentration behavior. When the strain reaches 15%, the composite structure becomes looser. At the same time, the larger strain causes the separation of epoxy and graphene. In the 1d model, CNTs are in contact to graphene surface and there is strong π-π interaction between benzene rings. As the strain reaches 30%, CNT adsorbs on graphene surface and separate from the epoxy matrix. For 2d and 3d models, the distances between CNT and graphene are 6.8 Å and 10.2 Å, respectively, and the attraction of them is weak. Thus, epoxy segments will coat CNT and graphene surfaces completely, leading to the separation between CNT and graphene at larger strain. In initial configurations of 2d and 3d models, the epoxy segments between CNT and graphene form a stable adsorption layer. Those epoxy segments are attracted by both CNT and graphene. During the tensile process, this fraction of epoxy segments gradually extends to connect CNT and graphene. In the 3d model, the interfacial adsorption region becomes larger and there are more epoxy segments between CNT and graphene. Thus, the mechanical property of the composite in the radial direction of CNT becomes better.
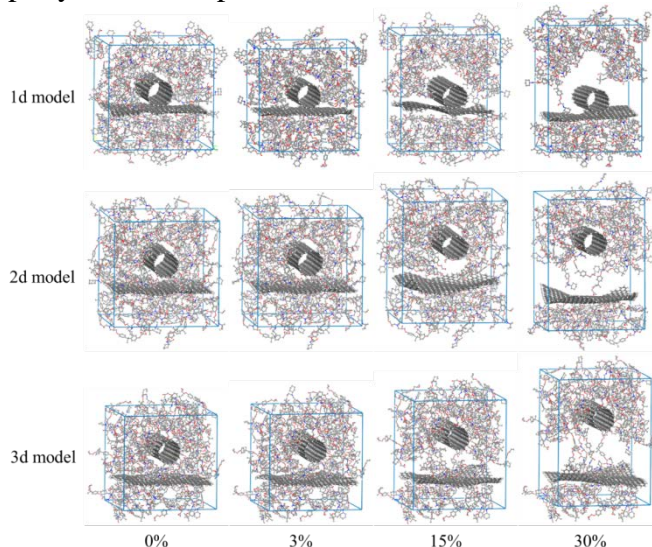

Figure 6. Snapshots of composites containing different d values with strain increasing from 0 to 30%

4. Conclusions

In summary, the effects of the CNT length and the distance of CNT and graphene on the mechanical property of the CNT/graphene/epoxy composite are investigated. Through uniaxial tensile simulations of the composites, we find that with the increase of CNT length, the epoxy adsorption layer on CNT surface increases, leading to the enhancement of system tensile property on the axial direction of CNT. The larger distance between CNT and graphene in the composite promotes the formation of an adsorption layer, which contributes to the improve of the composite mechanical property on the axial direction of CNT. The stretching of the composite on the radial direction of CNT shows that the epoxy adsorption layer between CNT and graphene acts as a bridging layer of them. The greater the distance between CNT and graphene, the better tensile property of the composite will be. The failure of composites under large strain is mainly caused by the separation between epoxy matrix and graphene interface.

Acknowledgments

References

[1] Dey, A.; Bajpai, O.P.; Sikder, A.K.; et al. Renew. Sust. Energy Rev. 2016, 53, 653–671.

[2] Hu, H.; He, Y.; Long, Z.; Zhan, Y. Polym. Adv. Technol. 2017, 28, 754–762.

[3] Min, C.; Liu, D.; Shen, C.; Zhang, Q.; Song, H.; Li, S.; Shen, X.; Zhu, M.; Zhang, K. Tribol. Int. 2018, 117, 217–224.

[4] Sumfleth, J.; Adroher, X.C.; Schulte, K. J. Mater. Sci. 2009, 44, 3241–3247.

[5] Yang, S.Y.; Lin, W.N.; Huang, Y.L.; Tien, H.W.; Wang, J.Y.; Ma, C.C.M.; Li, S.M.; Wang, Y.S. Carbon 2011, 49, 793–803.

[6] Kim, J.; Cote, L.J.; Kim, F.; Yuan, W.; Shull, K.R.; Huang, J. J. Am. Chem. Soc. 2010, 132, 8180–8186.

[7] Zhang, C.; Ren, L.; Wang, X.; Liu, T. J. Phys. Chem. C. 2010, 114, 11435–11440.

[8] Li, Y.; Yang, T.; Yu, T.; Zheng, L.; Liao, K. J. Mater. Chem. 2011, 21, 10844–10851.

[9] Shen, X.J.; Pei, X.Q.; Liu, Y.; Fu, S.Y. Compos. Part B Eng. 2014, 57, 120–125.

[10] Zhang, H.; Zhang, G.; Tang, M.; Zhou, L.; Li, J.; Fan, X.; Shi, X.; Qin, J. Chem. Eng. J. 2018, 353, 381–393.

[11] Sa, K.; Mahakul, P.C.; Subramanyam, B.V.R.S.; Raiguru, J.; Das, S.; Alam, I.; Mahanandia, P. IOP Conf. Ser. Mater. Sci. Eng. 2018, 338, 012055.

[12] Inuwa, I.M.; Arjmandi, R.; Ibrahim, A.N.; Mohamad Haafiz, M.K.; Wong, S.L.; Majeed, K.; Hassan, A. Fibers Polym. 2016, 17, 1657–1666.

[13] Pradhan, B.; Srivastava, S.K. Polym. Int. 2014, 63, 1219–1228.

[14] Jang, C.; Lacy, T.E.; Gwaltney, S.R.; Toghiani, H.; Pittman, C.U. Polymer 2013, 54, 3282–3289.

[15] Yuan, X.; Zhu, B.; Cai, X.; Qiao, K.; Zhao, S.; Yu, J. Appl. Surf. Sci. 2018, 458, 996–1005.

[16] Liu, F.; Hu, N.; Ning, H.; Atobe, S.; Yan, C.; Liu, Y.; Wu, L.; Liu, X.; Fu, S.; Xu, C.; et al. Carbon 2017, 115, 694–700.

[17] Zhang, Y.; Zhuang, X.; Muthu, J.; Mabrouki, T.; Fontaine, M.; Gong, Y.; Rabczuk, T. Compos. Part B-Eng. 2014, 63, 27–33.

[18] Sun, H. J. Phys. Chem. B 1998, 102, 7338–7364.

[19] Wu, T.T.; Xue, Q.Z.; Li, X.F.; Tao, Y.H.; Jin, Y.K.; Ling, C.C.; Lu, S.F. J. Supercrit. Fluids 2016, 107, 499–506.

[20] Arash, B.; Wang, Q.; Varadan, V.K. Sci. Rep. 2014, 4, 6479.

[21] Zheng, Q.B.; Xue, Q.Z.; Yan, K.Y.; Hao, L.Z.; Li, Q.; Gao, X.L. J. Phys. Chem. C 2007, 111, 4628–4635.

[22] Asche, T.S.; Behrens, P.; Schneider, A.M. J. Sol-Gel Sci. Technol. 2016, 81, 195–204.